JCS ePress online publication date 30 January 2007

IQGAP1 regulates cell motility by linking growth factor signaling to actin assembly

Lorena B. Benseñor[1], Ho-Man Kan[1], Ningning Wang[2], Horst Wallrabe[1], Lance A. Davidson[3], Ying Cai[1], Dorothy A. Schafer[1,2] and George S. Bloom[1,2,*]

Departments of [1]Biology and [2]Cell Biology, University of Virginia, Charlottesville, VA 22904, USA
[3]Department of Bioengineering, University of Pittsburgh, Pittsburgh, PA 15261, USA
*Author for correspondence (e-mail: gsb4g@virginia.edu)

Accepted 8 December 2006
Journal of Cell Science 120, 658-669 Published by The Company of Biologists 2007
doi:10.1242/jcs.03376

Summary

IQGAP1 has been implicated as a regulator of cell motility because its overexpression or underexpression stimulates or inhibits cell migration, respectively, but the underlying mechanisms are not well understood. Here, we present evidence that IQGAP1 stimulates branched actin filament assembly, which provides the force for lamellipodial protrusion, and that this function of IQGAP1 is regulated by binding of type 2 fibroblast growth factor (FGF2) to a cognate receptor, FGFR1. Stimulation of serum-starved MDBK cells with FGF2 promoted IQGAP1-dependent lamellipodial protrusion and cell migration, and intracellular associations of IQGAP1 with FGFR1 – and two other factors – the Arp2/3 complex and its activator N-WASP, that coordinately promote nucleation of branched actin filament networks. FGF2 also induced recruitment of IQGAP1, FGFR1, N-WASP and Arp2/3 complex to lamellipodia. N-WASP was also required for FGF2-stimulated migration of MDBK cells. In vitro, IQGAP1 bound directly to the cytoplasmic tail of FGFR1 and to N-WASP, and stimulated branched actin filament nucleation in the presence of N-WASP and the Arp2/3 complex. Based on these observations, we conclude that IQGAP1 links FGF2 signaling to Arp2/3 complex-dependent actin assembly by serving as a binding partner for FGFR1 and as an activator of N-WASP.

Supplementary material available online at
http://jcs.biologists.org/cgi/content/full/120/4/658/DC1

Key words: Cell motility, IQGAP, Actin, FGF, N-WASP, Arp2/3 complex

Introduction

IQGAP1 (Weissbach et al., 1998) is an ~380 kDa homodimeric protein (Bashour et al., 1997) that is widely expressed among vertebrate cell types from early embryogenesis (Cupit et al., 2004; Yamashiro et al., 2003) through adulthood (Bashour et al., 1997; Takemoto et al., 2001; Yamaoka-Tojo et al., 2004; Zhou et al., 2003). Several sequentially arranged functional domains enable IQGAP1 to bind directly to a rich spectrum of cytoskeletal, adhesion and regulatory proteins (Briggs and Sacks, 2003; Mateer and Bloom, 2003), including F-actin (Bashour et al., 1997; Fukata et al., 1997), the microtubule plus end capping protein, CLIP-170 (Fukata et al., 2002), E-cadherin (Kuroda et al., 1998), β-catenin (Kuroda et al., 1998), activated forms of the small G proteins, Cdc42 and Rac1 (Hart et al., 1996; Kuroda et al., 1996), calmodulin (Mateer et al., 2002), MAP kinases (Roy et al., 2004; Roy et al., 2005), the tumor suppressor protein, APC (Watanabe et al., 2004), and VEGFR2, the type 2 receptor for vascular endothelial growth factor, or VEGF (Yamaoka-Tojo et al., 2004). Like many of its associating proteins, IQGAP1 preferentially accumulates in the cell cortex, where it is most concentrated at actin filament-rich sites, such as lamellipodia and cell-cell junctions (Bashour et al., 1997; Hart et al., 1996; Kuroda et al., 1998; Yamashiro et al., 2003).

Regulation of cell motility and morphogenesis are among the most conspicuous cell biological functions of IQGAP1. The principal evidence for this conclusion is that siRNA-mediated knockdown of IQGAP1 potently inhibited cell motility (Mataraza et al., 2003; Yamaoka-Tojo et al., 2004), whereas cell migration (Mataraza et al., 2003) and neurite outgrowth (Li et al., 2005) were enhanced in cells overexpressing IQGAP1. Regulation of cell motility upstream of IQGAP1 has not been widely explored, but IQGAP1-dependent motility of endothelial cells was found to be triggered by binding of VEGF to VEGFR2, and subsequent recruitment of IQGAP1 to the cytoplasmic tail of VEGFR2 (Yamaoka-Tojo et al., 2004). Binding of a specific extracellular ligand to its cognate cell surface receptor thus represents at least one mechanism by which IQGAP1 can promote cell motility.

Knowledge of the downstream pathways by which IQGAP1 regulates cell motility has remained equally limited. One possible mechanism involves IQGAP1-dependent regulation of intercellular adhesion. IQGAP1 has been reported to inhibit cell-cell adhesion by binding to E-cadherin and β-catenin, thereby blocking interaction of β-catenin with α-catenin and uncoupling the adhesion machinery from the actin cytoskelelon (Kuroda et al., 1998). This inhibition of cell-cell adhesion by IQGAP1 can be overcome by binding of GTP-Cdc42 or GTP-Rac1 to IQGAP1, which dissociates IQGAP1 from E-cadherin and β-catenin (Fukata et al., 1999). At least one other potential explanation for the role of IQGAP1 in cell motility is well worth considering. The direct binding of IQGAP1 to F-actin in vitro (Bashour et al., 1997; Fukata et al.,

1997) and its extensive colocalization with actin filaments in lamellipodia (Bashour et al., 1997; Yamashiro et al., 2003) could reflect a role for IQGAP1 in controlling cell motility through regulation of actin dynamics. The force for lamellipodial protrusion, and by extension, cell motility, is provided by assembly of branched actin filament networks at the leading edges of motile cells. Assembly of these networks is thought to involve the Arp2/3 complex (Machesky et al., 1994) to nucleate new filaments from the sides of pre-existing filaments, and activators of the Arp2/3 complex, such as neural Wiskott-Aldrich Syndrome protein (N-WASP), WASP and the WAVE proteins, which themselves require activation by additional factors (Pollard and Borisy, 2003).

The study described here employed a combination of cell biological, biochemical and biophysical approaches to determine if regulation of cortical actin assembly by IQGAP1 underlies its critical role in cell motility. We demonstrate that IQGAP1 is part of the molecular machinery that stimulates branched actin filament nucleation and lamellipodial protrusion, and present evidence that activation of growth factor receptors is a common mechanism to engage this function of IQGAP1. Furthermore, because numerous proteins involved in promoting branched actin filament assembly failed to accumulate at the cell surface following receptor activation of IQGAP1-depleted cells, our results suggest that IQGAP1 coordinates the recruitment and activation of these proteins at the leading edge of motile cells.

Results

FGF2 stimulates cell motility through IQGAP1

To test the hypothesis that IQGAP1 regulates actin filament dynamics in response to activation of cell surface receptors other than VEGFR2, we began by examining motility of Madin-Darby bovine kidney (MDBK) cells stimulated with fibroblast growth factor 2 (FGF2). We chose FGF2 for this study because one of its principal receptors is FGFR1, whose cytoplasmic domain contains a region with 55% amino acid identity to the IQGAP1-binding region of VEGFR2 (Yamaoka-Tojo et al., 2004). Cell motility was induced in serum-starved MDBK cells by FGF2, and found to be tightly coupled to IQGAP1 expression. Wounds were scraped into confluent monolayers of serum-starved cells that had been treated with siRNA to reduce IQGAP1 protein levels to ~20% of normal (Fig. 1A) and FGF2 was added to the cultures 2 hours later. As shown by phase contrast microscopy in Fig. 1B (also see Fig. 5C for quantification), within 7 hours after introduction of FGF2, nearly full wound closure was observed in control cultures treated with scrambled RNA (scrRNA), but wounds scraped in confluent cultures of IQGAP1-depleted cells closed only partially. Most wound closure in control cultures was dependent on FGF2, because broad wounds persisted for more than 24 hours in cultures that were not stimulated with FGF2. We thus conclude that FGF2 stimulates migration of MDBK cells through a pathway that requires IQGAP1.

The impaired ability of IQGAP1-depleted cells to migrate in the wound healing assay resulted from a dramatic inhibition of FGF2-stimulated lamellipodial dynamics. Cells that had been treated with IQGAP1 siRNA or scrRNA were subcultured at low density, allowed to attach and spread on coverslips in serum-containing medium overnight, transferred to serum-free medium for 18 hours, and finally stimulated with FGF2.

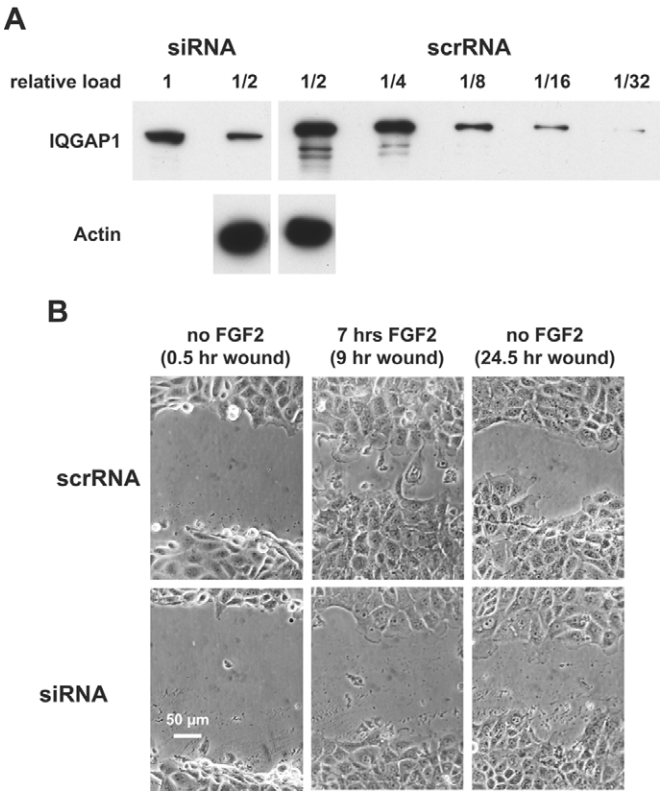

Fig. 1. IQGAP1 is required for FGF2-stimulated migration of MDBK cells. (A) MDBK cells were transfected with IQGAP1-specific siRNA or scrambled RNA (scrRNA) using a Nucleofector. To allow direct visual comparison of IQGAP1 levels in the two samples by western blotting, a concentration series of each cell extract was analyzed at the indicated relative dilutions. Note that siRNA reduced the IQGAP1 level to ~20% of normal, but had no effect on cellular actin content. (B) Confluent monolayers were then serum-starved for 8 hours, wounded with a micropipette tip, and 2 hours later were stimulated with 25 ng/ml FGF2. Note that movement of IQGAP1-depleted cells into the wound, as seen after 7 hours of FGF2 exposure, was severely impaired, and that broad wounds persisted for more than 24 hours after wounding in both scrRNA-treated and IQGAP1-depleted cells that were not stimulated with FGF2.

Images of individual cells that were not in direct contact with any neighboring cells were recorded by time-lapse, phase contrast microscopy before and after FGF2 stimulation. Timelines of lamellipodial protrusion and retraction were displayed as kymographs (Hinz et al., 1999), which facilitated visual and quantitative comparisons of lamellipodial behavior in cells containing normal versus diminished levels of IQGAP1. Typical kymographs are shown in Fig. 2A. The control cell kymograph demonstrated a high density of sharp, steadily advancing narrow peaks, each of which represented a rapid cycle of lamellipodial protrusion and retraction that resulted in net forward movement of the cell margin. By comparison, the kymograph of the IQGAP1-depleted cell contained only a few, much broader peaks, and indicated little, if any advance of the cell margin.

The impression obtained from this representative pair of kymographs was reinforced by quantitative analysis of three

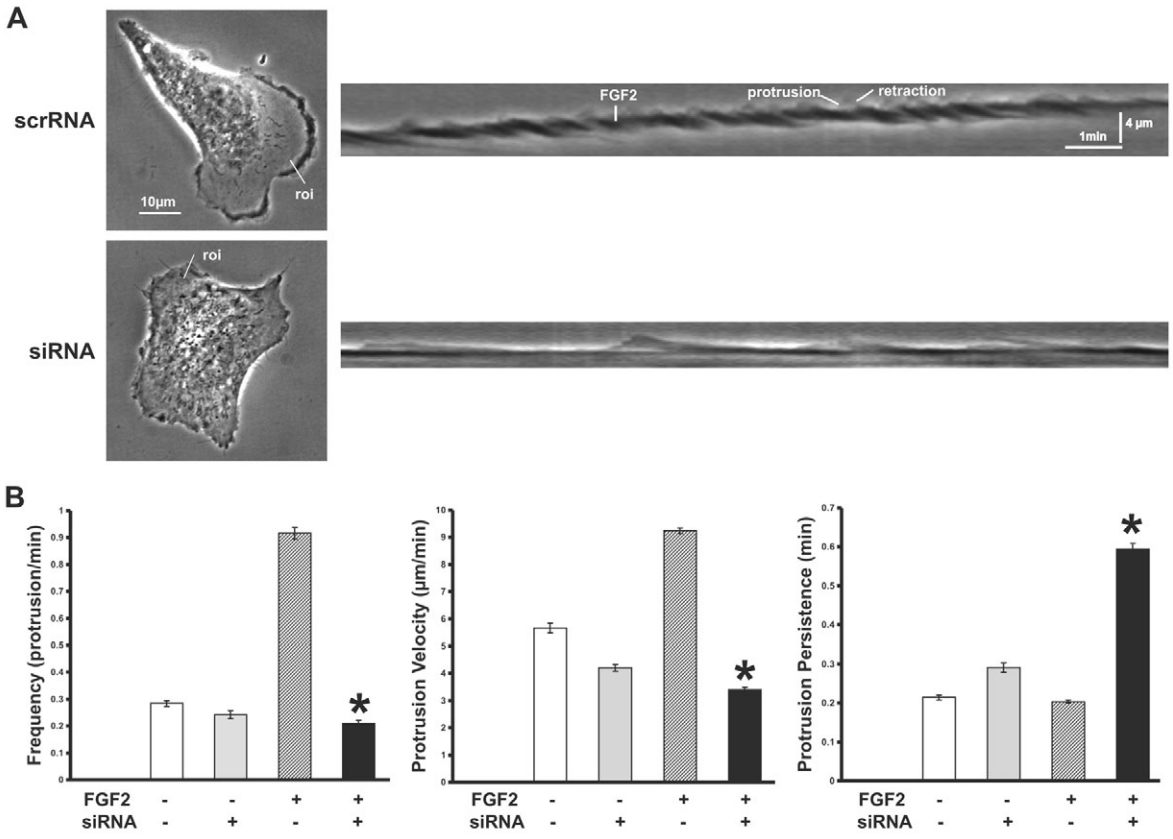

Fig. 2. Reduced lamellipodial dynamics in IQGAP1-depleted cells. Individual cells in sparse cultures that were serum-starved for 18 hours were imaged by phase contrast, time-lapse microscopy for 5 minutes before FGF2 was added to a final concentration of 25 ng/ml, and for 10 minutes thereafter. (A) Kymographic images (right panels) obtained from the indicated regions of interest (roi) at the margins of individual cells (left panels) treated with scrRNA or siRNA. Note how dynamic and motile the cell margin was in the control, scrRNA-treated cells compared to the cell depleted of IQGAP1 with siRNA. (B) Comparative responses of scrRNA-treated control (–) and IQGAP1 siRNA-treated (+) cells to FGF2 stimulation. The three parameters of lamellipodial dynamics that were measured before and after FGF2 stimulation were frequency, velocity and persistence of protrusion. The raw data were obtained from 180 regions of interest (roi) in 19 scrRNA-treated control cells, and from 180 roi in 21 siRNA-treated cells. Error bars indicate s.e.m. Differences between groups were analyzed using a one-way ANOVA test. Statistically significant differences at α=0.001 are indicated by * for control versus siRNA-treated cells after FGF2 exposure (see supplementary material Table S1 for detailed statistics, including post-hoc comparisons). The net conclusion is that control cells, but not IQGAP1-deficient cells, respond to FGF2 by making more dynamic lamellipodia.

distinct parameters of lamellipodial dynamics: the frequency of forming protrusions, the velocity with which protrusions advanced, and the persistence of protrusions (Fig. 2B; and for detailed statistics, including post-hoc comparisons, see supplementary material, Table S1). Comparison of control and IQGAP1-depleted cells prior to FGF2 stimulation indicated that their protrusion frequencies were indistinguishable, but that protrusions in control cells had a 34% higher velocity and a 39% lower persistence.

After FGF2 stimulation, lamellipodial behavior was strikingly different between control and IQGAP1-depleted cells. Addition of FGF2 to control cells caused protrusion frequency and velocity to increase by 224% and 64%, respectively, but protrusion persistence was unchanged. By contrast, addition of FGF2 to IQGAP1-depleted cells did not change the frequency of protrusions or their velocity, but did cause protrusion persistence to increase by 105%. Loss of IQGAP1, therefore, potently inhibited the ability of FGF2 to induce protrusions and increase the speeds at which they advanced, but caused protrusions that were able to form following FGF2 stimulation to be more long lasting. Despite this increased protrusion persistence, the net result of knocking down IQGAP1 was to prevent FGF2 from inducing productive protrusions. It is likely that the relatively inactive lamellipodia in IQGAP1-deficient cells stimulated with FGF2 accounted for their reduced migration in wound healing assays (Fig. 1B and Fig. 5C).

FGF2 induces intracellular association of IQGAP1 with N-WASP, the Arp2/3 complex and FGFR1

Because waves of lamellipodial protrusion are associated with periods of actin assembly (Pollard and Borisy, 2003), and IQGAP1 concentrates in lamellipodia and binds F-actin (Bashour et al., 1997), we investigated whether proteins that regulate actin assembly associated with IQGAP1 after FGF2 stimulation. IQGAP1 was immunoprecipitated from low-density cultures containing islands of relatively small numbers of cells (approximately 10-100 cells per island) before FGF2

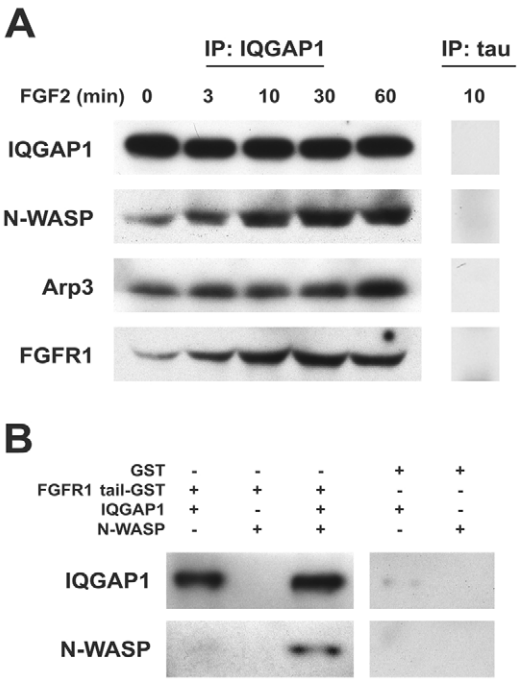

Fig. 3. FGF2 stimulates recruitment of IQGAP1, N-WASP, Arp2/3 complex and FGFR1 to lamellipodia. (A) Low-density cultures of serum-starved MDBK cells were stimulated with FGF2, and lysed at various times thereafter. At each indicated time point, IQGAP1 was immunoprecipitated out of the lysates with monoclonal anti-IQGAP1, and the immunoprecipitates were analyzed by immunoblotting with antibodies to IQGAP1 (polyclonal), N-WASP, Arp3 and FGFR1. As a control for non-specific immunoprecipitation, the tau-1 monoclonal antibody to tau, which is not expressed in MDBK cells, was substituted for monoclonal anti-IQGAP1, 10 minutes after FGF2 stimulation. Note that the IQGAP1 immunoprecipitates contained time-dependent increases in the levels of coimmunoprecipitated N-WASP, Arp3 and FGFR1, and that none of the proteins assayed by western blotting were immunoprecipitated by anti-tau. (B) Glutathione-Sepharose 4B beads were loaded with a fusion protein of the FGFR1 cytoplasmic tail coupled to GST, or to GST alone, and the beads were then mixed with IQGAP1, N-WASP, or both, and finally immunoblotting was used to detect any IQGAP1 or N-WASP that may have bound to the beads. Immunoblotting demonstrated direct binding of IQGAP1 and indirect, IQGAP1-dependent association of N-WASP with GST-FGFR1 tail, but not with GST.

stimulation and at various time points thereafter. As a control for non-specific immunoprecipitation, the tau-1 an antibody to tau, which is not expressed in MDBK cells, was substituted for anti-IQGAP1 10 minutes after FGF2 stimulation. The IQGAP1 immunoprecipitates contained time-dependent increases in coimmunoprecipitated N-WASP, Arp3 and FGFR1 beginning as early as 10 minutes after FGF2 stimulation, but none of the proteins assayed by western blotting were immunoprecipitated by anti-tau (Fig. 3A). Arp3 is a subunit of the Arp2/3 complex (Machesky et al., 1994), which coordinates with N-WASP to assemble branched actin filament networks (Pollard and Borisy, 2003). WAVE2, a different Arp2/3 complex activator that has been implicated specifically in lamellipodial protrusion (Yamazaki et al., 2003; Yan et al., 2003), was readily detectable in MDBK cell lysates by immunoblotting, but did not coimmunoprecipitate with IQGAP1 before or after FGF2 stimulation of serum-starved cells (not shown). Using purified proteins for in vitro binding assays, we determined that IQGAP1 binds directly to the cytoplasmic domain of FGFR1 and to N-WASP, and acts as a bridge for indirect association of FGFR1 and N-WASP (Fig. 3B and Fig. 8C).

Low-density MDBK cultures were also stained by double fluorescence microscopy for IQGAP1 plus FGFR1, N-WASP, Arp3 or F-actin. As shown in Fig. 4, FGF2 induced recruitment of IQGAP1 and the other four proteins to lamellipodia, where they colocalized extensively. These results place IQGAP1 predominantly within a cortical region where actin filament nucleation occurs and FGFR1 accumulates beyond basal levels following FGF2 stimulation. In FGF2-stimulated cells depleted of IQGAP1 with siRNA, however, FGFR1, N-WASP and Arp3 were not recruited to the cortex, and F-actin-rich lamellipodia failed to form.

Impaired wound healing by N-WASP-depleted MDBK cells

The evidence presented to this point raised the possibility that N-WASP, like IQGAP1, is required in MDBK cells for FGF2-stimulated lamellipodial protrusion and cell motility. To test this hypothesis, MDBK cells were depleted of N-WASP with siRNA, and tested for FGF2-stimulated wound healing. As illustrated in Fig. 5, wound healing in N-WASP-deficient cultures was severely impaired, and quantitatively similar to the poor wound healing observed in IQGAP1-depleted cultures. Thus, in contrast to other cellular systems in which WAVE2 was found to support lamellipodial advance (Yamazaki et al., 2003; Yan et al., 2003), FGF2-stimulated lamellipodial protrusion in MDBK cells requires N-WASP.

IQGAP1 stimulates branched actin filament nucleation through N-WASP and the Arp2/3 complex

The requirement for both IQGAP1 and N-WASP for FGF2-dependent cell migration, and for intracellular association of IQGAP1, N-WASP and the Arp2/3 complex suggested that these three factors work in concert to stimulate actin filament nucleation. This hypothesis was verified using a spectrofluorometric assay for assembly of pyrene-labeled actin (Bryan and Coluccio, 1985) (Fig. 6A). In the presence of 1.3 μM actin, 50 nM Arp2/3 complex and 50 nM N-WASP, the maximum actin assembly rate (V_{max}) and shortest lag time to reach V_{max} was achieved at an IQGAP1 concentration of 30 nM. Compared to samples containing 30 nM IQGAP1, control samples that lacked IQGAP1 assembled with an ~50% slower V_{max} and took four to five times longer to reach V_{max}. Lesser stimulation of actin assembly, or none at all, was observed at lower and higher IQGAP1 concentrations. IQGAP1 thus stimulates actin nucleation by the Arp2/3 complex and N-WASP, but within a narrow concentration range, suggesting that the effects of IQGAP1 on actin assembly reflect a concentration-dependent balance between stimulatory and inhibitory activities. Similar results were obtained at Arp2/3 complex concentrations of 30-100 nM, and at N-WASP concentrations of 30-350 nM (as in Fig. 7A). IQGAP1 did not stimulate actin assembly appreciably in the absence of other factors, and stimulation required the presence of both the Arp2/3 complex and N-WASP (Fig. 6B).

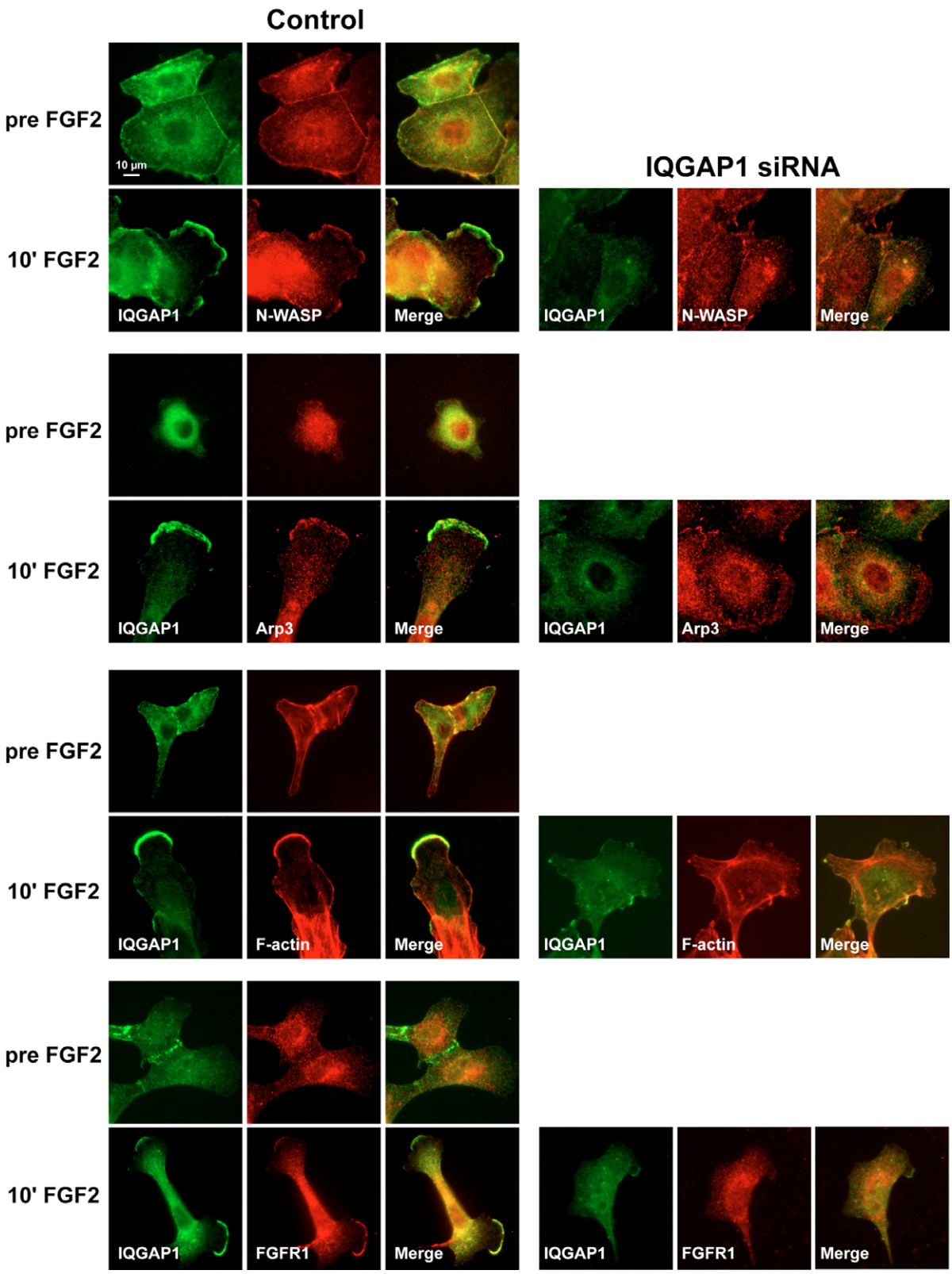

Fig. 4. IQGAP1-dependent recruitment of N-WASP, Arp3 and FGFR1 to the cell periphery after FGF2 stimulation. Immunofluorescence microscopy revealed co-recruitment and colocalization of IQGAP1, N-WASP, Arp3 and FGFR1 to lamellipodia after FGF2 stimulation for 10 minutes, of low-density cultures of serum-starved MDBK cells containing IQGAP1 (Control cells). FGF2 was unable to recruit N-WASP, Arp3 and FGFR1 to cell margins in IQGAP1-deficient, siRNA-treated cells. To improve visualization of cell margins and intracellular details in IQGAP1-depleted cells, micrograph exposures for the siRNA samples were twice as long in the TRITC channel and 4.5 times longer in the FITC channel as they were for the scrRNA samples.

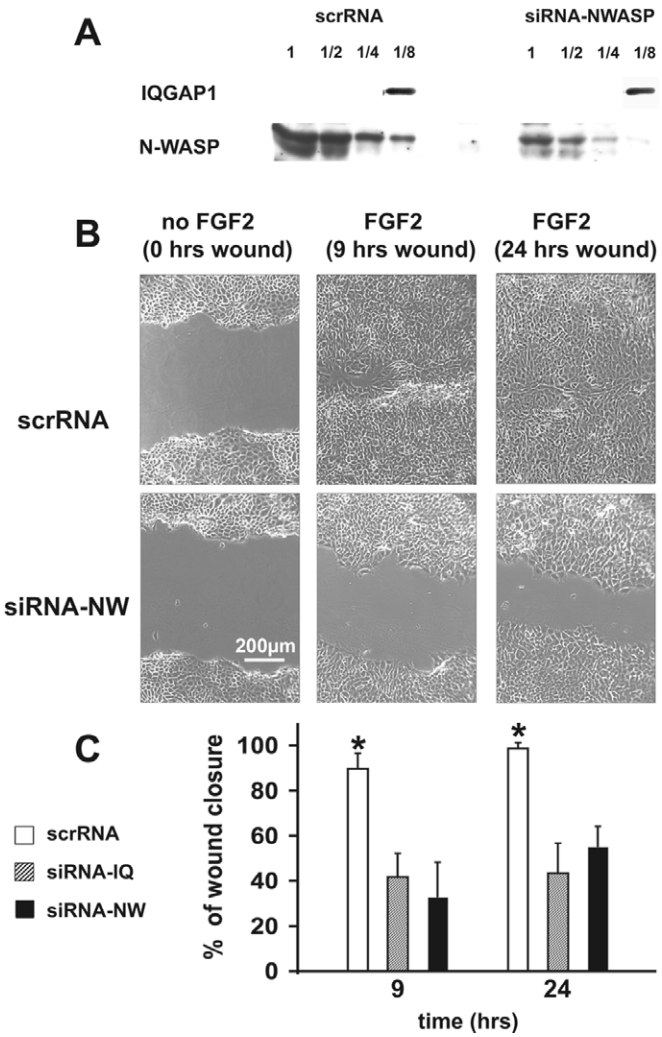

Fig. 5. N-WASP is required for FGF2-stimulated migration of MDBK cells. (A) MDBK cells were transfected with N-WASP-specific siRNA or scrambled RNA (scrRNA) using a Nucleofector. To allow direct visual comparison of N-WASP levels in the two samples by western blotting, a concentration series of each cell extract was analyzed at the indicated relative dilutions. Note that siRNA reduced the N-WASP level to ~1/3 of normal, but had no effect on cellular IQGAP1 content. (B) Confluent monolayers were then serum-starved for 8 hours, wounded with a micropipette tip, and 2 hours later were stimulated with 25 ng/ml FGF2. Note that movement of N-WASP-depleted cells into the wound after 9 or 24 hours of FGF2 exposure was severely impaired. (C) Percentage of wound closure was quantified by measuring the average width of eight randomly chosen regions of interest of each wound at 0, 9, and 24 hours after FGF2 addition. Data are expressed relative to the average wound widths at 0 hours. Error bars indicate standard deviations for three experiments, and asterisks (*), indicate significant differences between scrRNA controls and corresponding siRNA-treated cultures at $\alpha<0.001$.

Taken together, these results establish IQGAP1 as a novel activator of N-WASP.

Confirmation that IQGAP1 promoted branched actin filament nucleation was obtained by direct visualization of actin polymerization stimulated by IQGAP1 in the presence of the Arp2/3 complex and N-WASP, by total internal reflection fluorescence (TIRF) microscopy (Kuhn and Pollard, 2005) (Fig. 6C and supplementary material, Movie 1). The rates at which total filament length increased with or without IQGAP1 were similar until ~100 seconds, when the rate began to increase more rapidly in the IQGAP1-containing sample (Fig. 6D). The time point for this transition was also marked by a large increase in the rate at which filament branches appeared in the IQGAP1-containing sample. Indeed, by plotting the number of branches per μm of filament length as a function of time, it became apparent that after 100 seconds of assembly, the density of branches in the presence of IQGAP1 was four- to fivefold higher than in its absence, relatively constant with time for the next 500 seconds, and comparable to what was observed when an optimal concentration of GTP-bound Cdc42, a robust N-WASP activator (Rohatgi et al., 2000; Rohatgi et al., 1999), was used in place of IQGAP1 (Fig. 6E). These results confirm and extend the conclusion from spectrofluorometric assays (Fig. 6A) that IQGAP1 stimulates branched actin filament nucleation by activating N-WASP, and by extension, the Arp2/3 complex.

In addition to binding and activating N-WASP, GTP-activated Cdc42 binds directly to IQGAP1 (Hart et al., 1996; Kuroda et al., 1996; McCallum et al., 1996). We therefore compared the ability of activated Cdc42 and IQGAP1, individually and together, to stimulate actin assembly (Fig. 7A). In the presence of 2 μM actin, 50 nM Arp2/3 complex and 350 nM N-WASP, optimal concentrations of activated Cdc42 (105 nM) and IQGAP1 (35 nM) promoted actin polymerization nearly identically. When both Cdc42 and IQGAP1 were present, however, the lag time before V_{max} was reached was dramatically reduced and the peak assembly rate increased additively. Similar results were obtained when the concentrations of actin, Arp2/3 complex and N-WASP were as low as 1.3 μM, 30 nM and 50 nM, respectively. IQGAP1 and activated Cdc42 can thus work in concert to drive especially rapid nucleation of actin filament branches.

To investigate why stimulation of actin assembly occurs within a narrow range of IQGAP1 concentrations (Fig. 6A and Fig. 8B), we monitored effects of IQGAP1 on assembly stimulated by the Arp2/3 complex plus the N-WASP VCA fragment, which constitutively activates the Arp2/3 complex (Rohatgi et al., 1999). As shown in Fig. 7B, IQGAP1 did not bind GST-VCA, but did exhibit dose-dependent inhibition of actin assembly in the presence of GST-VCA plus the Arp2/3 complex. By contrast, $IQGAP1_{\Delta NT}$, which lacks the first 156 N-terminal amino acids of full-length IQGAP1 and does not bind F-actin (see supplementary material Fig. S1), had no effect on actin assembly stimulated by GST-VCA and the Arp2/3 complex. These data suggest that high concentrations of full-length IQGAP1 are less effective at stimulating actin assembly by the Arp2/3 complex and N-WASP because of competition between IQGAP1 and the Arp2/3 complex for binding to existing actin filaments, where the Arp2/3 complex most efficiently nucleates new actin filaments.

Stimulation of actin assembly through N-WASP and the Arp2/3 complex was also observed for three progressively smaller N-terminal IQGAP1 fragments (Fig. 8A,B): $IQGAP1_{2\text{-}522}$, a homodimer that binds F-actin (Mateer et al., 2002), $IQGAP1_{2\text{-}210}$, an F-actin binding monomer (Mateer et al., 2004), and $IQGAP1_{2\text{-}71}$, a presumptive monomer that does

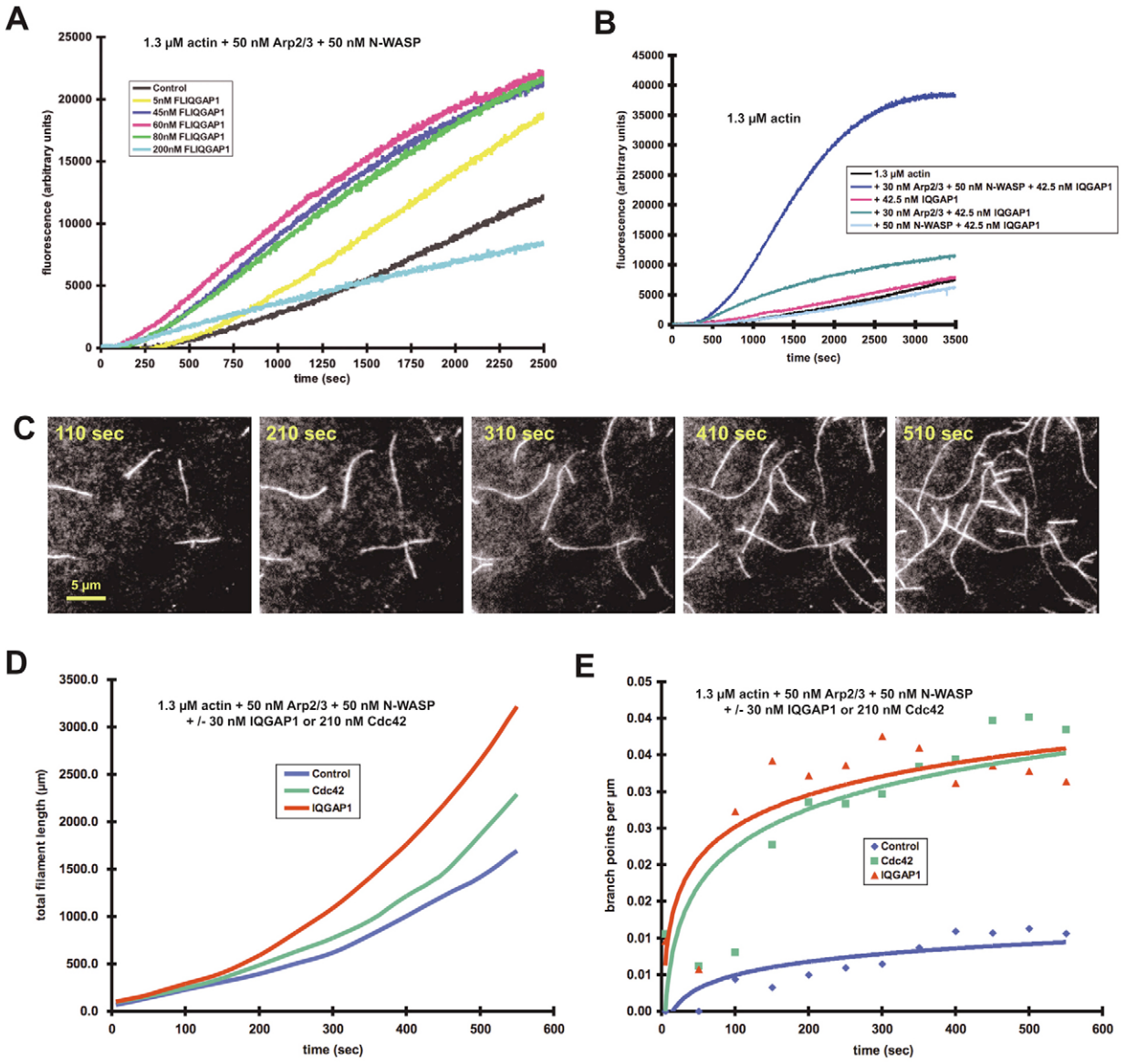

Fig. 6. Stimulation of branched actin filament assembly by IQGAP1. (A) Effects of IQGAP1 on actin (5% labeled with pyrene) assembly in the presence of N-WASP and the Arp2/3 complex were monitored using a pyrene-actin fluorescence assay. Note that maximal stimulation of assembly was achieved at 30 nM IQGAP1, and that higher and lower concentrations stimulated less or not at all. (B) Actin assembly stimulation by IQGAP1 requires N-WASP plus Arp2/3 complex. (C) IQGAP1-stimulated assembly of branched actin filament networks observed directly by TIRF microscopy. (D) Total lengths of actin filaments observed by TIRF microscopy were measured as a function of time, for samples containing or lacking IQGAP1 or activated Cdc42, a previously described for the N-WASP activator (Rohatgi et al., 1999). Maximum rates of actin assembly were achieved in the IQGAP1 sample. (E) The same micrographs were used to determine the number of filament branch points per μm of actin filament as a function of time. Note that the IQGAP1 and Cdc42 samples quickly attained a filament branch density four- to fivefold greater than the control sample that contained neither IQGAP1 nor Cdc42.

not bind F-actin (Mateer et al., 2004). By contrast, IQGAP1$_{\Delta NT}$ showed little evidence of assembly stimulation. Like full-length IQGAP1, each N-terminal fragment had an optimal concentration for stimulating the rate of actin assembly. The V_{max} for each fragment at its optimal concentration was similar to that observed for full-length IQGAP1, although the lag time before V_{max} was reached was much longer for the stimulatory fragments than for full-length IQGAP1 (Fig. 8B). We, therefore, conclude that several N-terminal fragments of IQGAP1 can stimulate actin assembly in the presence of the Arp2/3 complex and N-WASP, albeit not as well as full-length IQGAP1. Furthermore, this stimulatory activity of IQGAP1 does not require dimerization or binding to actin filaments.

Actin assembly stimulation in the presence of the Arp2/3 complex and N-WASP is well correlated with direct binding of IQGAP1 or IQGAP1 fragments to N-WASP. Purified, N-terminally his-tagged versions of full-length IQGAP1, IQGAP1$_{2-522}$, IQGAP1$_{2-210}$, IQGAP1$_{2-71}$, and IQGAP1$_{\Delta NT}$ were bound to nickel-agarose beads and mixed with purified N-WASP. Fig. 8C demonstrates that N-WASP bound

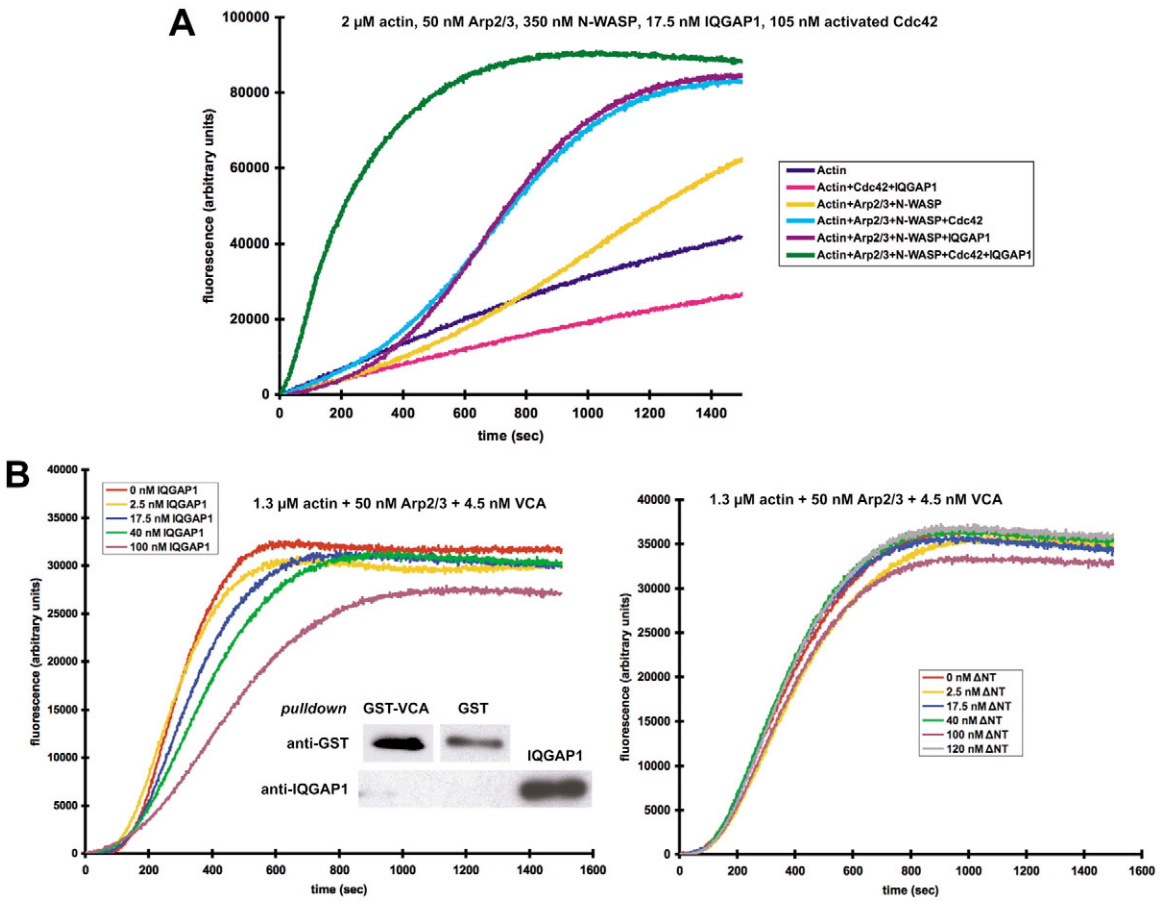

Fig. 7. Co-stimulation of actin assembly by IQGAP1 plus activated Cdc42, and inhibition of VCA-stimulated actin assembly by IQGAP1. (A) When used together, IQGAP1 and activated Cdc42 stimulated actin assembly rates additively, and virtually eliminated the lag period before peak assembly rates were reached using either IQGAP1 or activated Cdc42 alone. (B) In the presence of a GST-tagged, constitutively active, N-WASP VCA fragment, IQGAP1, but not IQGAP1$_{\Delta NT}$, caused dose-dependent inhibition of assembly.

specifically to all IQGAP1 proteins tested. These results establish the presence of an N-WASP binding region near the N terminus of IQGAP1, and imply that binding underlies N-WASP activation. The ability of IQGAP1$_{\Delta NT}$ to bind N-WASP, but its borderline ability to stimulate actin assembly indicates, however, that binding and activation of N-WASP are separable. Using similar nickel-agarose pull-down assays, we did not detect direct binding of IQGAP2 to the Arp2/3 complex (not shown).

Discussion

The collective data presented here suggest that activation of a cell surface receptor, FGFR1, by one of its extracellular ligands, FGF2, recruits IQGAP1 to the cortically localized cytoplasmic domain of the receptor. IQGAP1 then promotes branched actin filament nucleation through N-WASP and the Arp2/3 complex, and as a result, lamellipodial protrusion, in the immediate vicinity of activated receptors. This mechanism by which IQGAP1 serves as an intermediate between growth factor signaling, and cellular morphogenesis and motility likely applies to IQGAP1-dependent migration of endothelial cells stimulated by VEGF binding to VEGFR2 (Yamaoka-Tojo et al., 2004), and may apply to other growth factor-receptor pairs that await identification. A different member of the IQGAP family, IQGAP2, which is 62% identical in amino acid sequence to IQGAP1 (Brill et al., 1996), may use a related mechanism to trigger actin assembly and cellular morphogenesis in platelets. The filopodia and lamellipodia that platelets elaborate after thrombin activation may owe their formation to thrombin-induced macromolecular assemblies of IQGAP1, actin and the Arp2/3 complex (Schmidt et al., 2003).

A key question that remains unanswered is why suppression of IQGAP1 protein levels so dramatically reduces cell motility (Fig. 1 and Fig. 5C) (see also Mataraza et al., 2003; Watanabe et al., 2004; Yamaoka-Tojo et al., 2004) when several N-WASP-independent pathways for activating Arp2/3 complex-mediated cell motility are known to exist (Miki and Takenawa, 2003), and WAVE2 (Suetsugu et al., 2003; Yamazaki et al., 2003), rather than N-WASP (Benesch et al., 2005), is thought to be the principal Arp2/3 complex activator for lamellipodial advance. Among many possible explanations worth exploring are that specific receptor-ligand pairs, such as FGFR1-FGF2 and VEGFR2-VEGF, trigger Arp2/3 complex activation primarily through IQGAP1 and N-WASP, that N-WASP is not the only Arp2/3 complex activator that can be stimulated by IQGAP1, and that actin assembly stimulated by IQGAP1 indirectly supports lamellipodial protrusion. Regarding the last possibility, IQGAP1 knockdown may impair cell motility

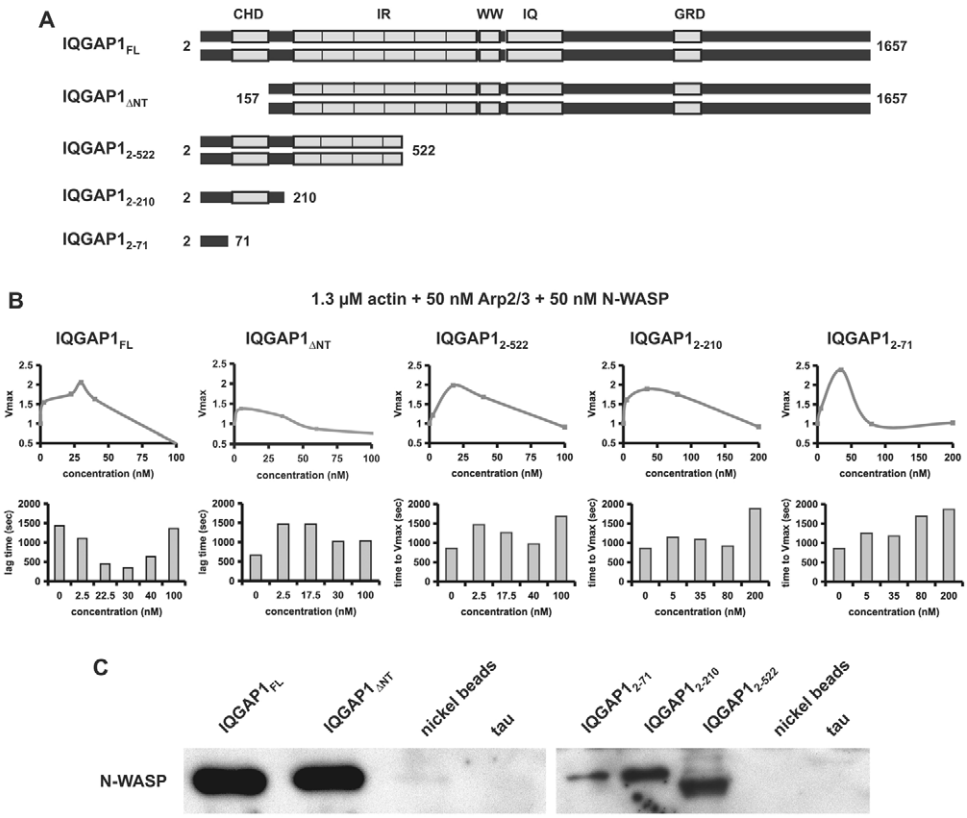

Fig. 8. IQGAP1 fragments stimulate actin assembly and bind N-WASP. (A) A schematic representation of functional domains present in recombinant full-length IQGAP1 and four fragments used for experiments documented here: CHD, F-actin-binding calponin homology domain; IR, IQGAP repeats that mediate homodimerization; WW, ERK2-binding WW domain; IQ, calmodulin-binding IQ motifs; GRD, GAP (GTPase activating protein)-related domain involved in binding activated Cdc42 and Rac1. All proteins were his-tagged at their N termini, and the diagrams indicate whether each protein is a monomer or homodimer in aqueous solution. (B) The pyrene actin assembly assay was used to evaluate each protein at several concentrations in the presence of 1.3 μM actin (5% pyrene-labeled), 50 nM N-WASP and 50 nM Arp2/3 complex. Shown here are the maximum velocities (V_{max}) of actin assembly (upper panels) and lag times before V_{max} was reached (lower panels). Note that optimal concentrations of all recombinant proteins, except IQGAP1$_{\Delta NT}$, supported a V_{max} approx. twofold higher than controls that contained only actin, N-WASP and Arp2/3 complex, but that the optimal concentration of full-length IQGAP1 (IQGAP1$_{FL}$) reached V_{max} at least twice as fast as the fragments. (C) N-WASP was mixed with nickel-agarose beads or nickel-agarose beads that were pre-loaded with recombinant, his-tagged IQGAP1$_{FL}$, IQGAP1$_{\Delta NT}$, IQGAP1$_{2-522}$, IQGAP1$_{2-210}$, IQGAP1$_{2-71}$, or tau as a negative control. Beads contained an approx. twofold molar excess of his-tagged proteins relative to N-WASP, and chemiluminescent immunoblotting was used to detect any N-WASP that may have bound to beads. Note the specific binding of N-WASP to all forms of IQGAP1 that were tested. The slightly increased electrophoretic mobility of N-WASP in the IQGAP1$_{2-522}$ pull-down assay probably represents a gel artefact caused by that fact N-WASP and IQGAP1$_{2-522}$ migrate nearly identically in SDS-PAGE.

because it reduces the levels of activated Cdc42 and Rac1 (Mataraza et al., 2003), which are known to stimulate the Arp2/3 complex indirectly through activation of WASP/WAVE proteins (Pollard and Borisy, 2003). Alternatively, receptor trafficking, which could be required for sustained cell migration in response to extracellular growth factors, may depend on actin assembly stimulated by IQGAP1. In favor of the receptor trafficking model is evidence that N-WASP, along with the Arp2/3 complex, is recruited to clathrin-coated pits as they invaginate, and is required for receptor-mediated endocytosis of EGF receptors (Benesch et al., 2005). Considering the ability of IQGAP1 to bind N-WASP directly (Fig. 8C) and to stimulate actin assembly through N-WASP and the Arp2/3 complex (Fig. 6), it is possible that IQGAP1 is necessary for normal FGFR1 trafficking, at least at the step of receptor endocytosis, which in turn might be required for formation of productive protrusions in cells stimulated by FGF2.

An equally attractive possibility concerns the mechanical strength of branched actin filament networks. IQGAP1 is a homodimeric protein that can crosslink actin filaments (Bashour et al., 1997) because it contains an F-actin binding calponin homology domain on each of its two identical subunits (Mateer et al., 2004). By joining N-WASP and the Arp2/3 complex in a supramolecular complex that nucleates actin filament branches, IQGAP1 may reside at the junction of mother and daughter filaments in branched filament networks, where it would be ideally positioned to crosslink mother and daughter filaments, and thus might provide branched filament networks with increased mechanical integrity. Fortifying filament networks in such a manner could allow filaments that are at the leading edge and anchored to the lamellipodial

network to push forward the plasma membrane more effectively as filament polymerization proceeds. We are not aware of any protein other than IQGAP1 that both stimulates branched actin filament nucleation through the Arp2/3 complex and crosslinks actin filaments. Thus, even if IQGAP1 was a relatively minor stimulator of the Arp2/3 complex in most cellular contexts, its actin filament crosslinking activity could be crucial for formation of productive lamellipodia.

Although direct binding of activated Cdc42 to N-WASP allows N-WASP to stimulate the actin filament nucleating activity of the Arp2/3 complex in vitro in the absence of additional factors (Rohatgi et al., 1999), other proteins could play very important roles in this process. For example, WASP-interacting protein (WIP)-mediated inhibition of N-WASP can be relieved by activated Cdc42, but in a manner dependent on forming binding protein 1-like (FNBP1L, also known as Toca-1), which binds both activated Cdc42 and N-WASP (Ho et al., 2004). By comparison, and as shown here, IQGAP1 can bind and stimulate N-WASP independently of activated Cdc42 (Fig. 6, Fig. 7A and Fig. 8C), but can also act cooperatively with activated Cdc42 to promote actin filament nucleation in vitro through N-WASP and the Arp2/3 complex (Fig. 7A). In the latter case, IQGAP1, like Toca-1, may engage activated Cdc42 and N-WASP as a complex that sustains a high level of filament formation at the leading edge of motile cells. The increased number of lamellipodial protrusions and their faster rate of forward extension after stimulation of MDBK cells with FGF2 are consistent with this idea. The fact that IQGAP1 depletion leads to reduced levels of activated Cdc42 and Rac1 in cells (Mataraza et al., 2003) provides additional support for this notion. Cdc42 binds IQGAP1 with 50-fold higher affinity than it binds WASP, a protein closely related to N-WASP (Zhang et al., 1997), so IQGAP1 could serve to anchor activated Cdc42 in close association with N-WASP. Finally, IQGAP1 and WASP interact with physically distinct regions of activated Cdc42 (Li et al., 1999), so maximal activation of N-WASP might be achieved by simultaneous interactions of activated Cdc42 with both IQGAP1 and N-WASP. Thus, a Cdc42-IQGAP1 complex, rather than Cdc42 and IQGAP1 acting independently, may be responsible for maintaining N-WASP-dependent and Arp2/3 complex-dependent protrusive activity.

On the other hand, binding of activated Cdc42 to IQGAP1 would also be expected to increase cell-cell adhesion by dissociating IQGAP1 from E-cadherin and β-catenin, and thereby strengthen the cadherin-catenin-actin connection that acts as a counterforce to cell migration (Kuroda et al., 1998). The apparent migration-promoting and cell-cell adhesion promoting activities of IQGAP1 are not necessarily in conflict, but it seems unlikely that decreased intercellular adhesion underlies IQGAP1-dependent cell motility induced by FGF2. On the contrary, assuming that one effect of FGF2 stimulation was an increase in IQGAP1-dependent intercellular adhesion, that effect must be overwhelmed by IQGAP1-dependent actin assembly and consequent lamellipodial protrusion induced by FGF2.

The failure of FGFR1, N-WASP and the Arp2/3 complex to be recruited to the cell cortex following FGF2 stimulation of IQGAP1-deficient cells (Fig. 4) indicates that IQGAP1 plays a far broader role in cell motility than merely stimulating actin filament nucleation. IQGAP1 also appears to recruit to the cell surface many key components of the motile machinery. This finding is reminiscent of recent reports that IQGAP1 integrates the actin and microtubule cytoskeletons by binding directly to both CLIP-170 and APC, which are microtubule plus end tracking proteins (Fukata et al., 2002; Watanabe et al., 2004). IQGAP1 may thus be a master organizer of signal transduction, cytoskeletal and cell adhesion molecules that act cooperatively to regulate cell motility and morphogenesis. We suggest in particular that the interaction of IQGAP1 with FGFR1 represents a critical step that bridges extracellular signals with cellular responses. IQGAP1 may establish or maintain FGF2-dependent signaling by regulating the polarized distribution of FGFR1 receptors at the cell surface. Through its F-actin binding activity, IQGAP1 may stabilize connections among cell surface FGFR1, cortical F-actin and the machinery that powers cell movement. In this regard, IQGAP1 and N-WASP may function to maintain FGFR1 homeostasis at the plasma membrane.

Materials and Methods

Antibodies

The following antibodies were used: primary mouse monoclonal anti-IQGAP1 (Mateer et al., 2002), anti-actin (Chemicon) and tau-1 (Binder et al., 1985), and rabbit polyclonal antibodies to IQGAP1 (Mateer et al., 2002), N-WASP (Santa Cruz), Arp3 (Welch et al., 1997) and FGFR1 (Santa Cruz). Secondary antibodies included goat anti-mouse IgG and goat anti-rabbit IgG labeled with FITC or TRITC (Southern Biotech, Birmingham, AL), goat anti-mouse IgG labeled with Alexa Fluor-647 (Molecular Probes), and goat anti-mouse IgG and goat-anti rabbit IgG labeled with horseradish peroxidase (KPL Inc., Gaithersburg, MD).

Cell culture, IQGAP1 and N-WASP knockdown, and wound healing

MDBK (Madin-Darby bovine kidney) epithelial cells were obtained from the American Type Culture Collection and maintained in Dulbecco's miminum essential medium (Gibco) plus 10% Cosmic calf serum (HyClone). siRNA for bovine IQGAP1 (target sequence: AAGGCTGAGCTGGTGAAACTG) and a scrambled (scrRNA) control (target sequence: AAGTACCAGGGACGTGAGTGT) were purchased from Qiagen as Alexa Fluor-647-labeled products. siRNA for N-WASP was purchased from Dharmacon (catalogue no. D-006444-06), and according to the manufacturer was directed against a human N-WASP sequence that is identical to the corresponding bovine N-WASP sequence. 2 μg of siRNA specific for IQGAP1 or N-WASP, or 2 μg of scrRNA were transfected into MDBK cells using a Nucleofector (Amaxa, Cologne, Germany) and the protocol specifically recommended by the manufacturer for MDBK cells (Nucleofector Kit R and program X-001). 48-72 hours after transfection, confluent monolayers of cells that were growing in 24-well dishes and had been serum starved for the previous 8 hours were wounded by scratching with a micropipette tip. The cells were allowed to recover for 2 hours, after which media were replaced with fresh media containing or lacking 25 ng/ml FGF2 (Sigma). Phase contrast micrographs of the cultures were taken within 30 minutes after wounding and at various times thereafter using Scion Image software (Scion, Frederick, MD) and a Cohu model 2222-1000 camera mounted on a Nikon Diaphot microscope with a Nikon 10×, 0.25 NA, phase 1 DL objective.

Kymographic analysis

MDBK cell cultures were transfected by nucleofection with scrRNA or siRNA and grown to confluence, after which 5×10^4 cells were subcultured onto 25 mm round, #1 thickness coverslips coated with 5 μg/ml fibronectin (Sigma), and grown overnight in serum-containing medium. The cells were then cultured for at least 14 hours in serum-free medium, and finally for 4 hours in Phenol-Red-free MEM containing 15 mM Hepes (Gibco). Following this MEM acclimation period, cells were imaged by time-lapse phase contrast microscopy at 12 frames per minute beginning 5 minutes before addition of 50 ng/ml FGF2, which occurred 48-72 hours after transfection. Images were captured without binning using a Hamamatsu Orca-ER 1.3 megapixel cooled CCD mounted on a Zeiss Axiovert S100 equipped with a Zeiss 63× 1.4 NA phase 3 planapochromatic objective. Cells were maintained on the microscope stage in Attofluor Cell Chambers (BD Bioscience, Rockville, MD) at 37°C in an atmosphere of 95% air plus 5% CO_2. OpenLab 4 software (Improvision) running on a Power Macintosh G4 computer (Apple) was used to control the camera and shutters, and to program the time-lapse parameters. NIH Image 1.62 public domain software (http://rsb.info.nih.gov/nih-image/) was used to generate kymographs of lamellipodia (Hinz et al., 1999) from user-specified regions of interest. Excel 2004 for Mac (Microsoft) was used to generate the bar graphs of protrusion frequency, velocity and persistence shown in Fig. 2B, and SPSS 11 for

Mac OS X statistical software (SPSS, Inc.) was used for one-way ANOVA (see supplementary material Table S1).

Fluorescence microscopy

Cells were fixed and permeabilized either by immersion for 5 minutes in methanol at –20°C, or by successive incubations in 4% ρ-formaldehyde in PBS (10 minutes) followed by 0.2% Triton X-100 (2 minutes). After fixation and permeabilization, cells were washed thoroughly and incubated successively with primary and secondary antibodies for 1 hour each, with several washes after each antibody step. F-actin was detected in ρ-formaldehyde-fixed, Triton X-100-permeabilized cells with Alexa Fluor 568-phalloidin (Molecular Probes). Fluorescence confocal micrographs were taken using a CARV spinning disk confocal head (Atto Instruments) mounted on the Zeiss microscope system described earlier.

Immunoprecipitation

Sub-confluent MDBK cells were serum starved for 12-18 hours, before being stimulated with 50 ng/ml FGF2. Cells harvested just prior to FGF2 addition and at various times thereafter were lysed in buffer A (50 mM Hepes pH 7.4, 50 mM NaCl, 0.5% sodium deoxycholate, 1 mM EDTA, 1% Triton X-100, 2 mM $NaVO_4$, 20 mM NaF, 1 mM PMSF, and 2 μg/ml each of chymostatin, leupeptin and pepstatin A), and the lysates were then clarified by centrifugation. Monoclonal anti-IQGAP1, or monoclonal tau-1 as an irrelevant control, was then added to the clarified lysates, which were subsequently incubated for 4 hours at 4°C. Next, EZview red protein-G affinity gel beads (Sigma) were added to samples, which were incubated for an additional 2 hours at 4°C. Immuno-complexes were collected by brief centrifugation, washed in buffer B (50 mM Tris pH 7.4, 150 mM NaCl, 0.5% Triton X-100, 1 mM PMSF), and analyzed by immunoblotting using polyclonal antibodies to IQGAP1, N-WASP, Arp3 and FGFR1, and SuperSignal chemiluminescent reagents (Pierce).

Affinity pull-down assay

Coding DNA for the FGFR1 cytoplasmic domain was amplified by PCR from mouse brain cDNA using the following primers: forward, 5′-gtcatc-atctataagatgaagagcggc-3′; reverse, 5′-ctcaggtaacggctcatgagagaagac-3′. *Eco*RI and *Not*I cloning sites were added by PCR using these primers: forward, 5′-gcgggaattcgtcatcatctaaga-3′; reverse, 5′-gaagcggccgcctcaggtaacgg-3′. GST-FGFR1 tail and unmodified GST were expressed in transformed *E. coli* (strain BL21), and purified from bacterial lysates using glutathione-Sepharose 4B beads (Pharmacia). Glutathione-Sepaharose 4B beads containing ~2 μM GST-FGFR1 tail or GST were then mixed with 1 μM $IQGAP1_{FL}$; Ni-NTA-agarose (nickel) affinity beads (Qiagen) containing ~1 μM his-tagged $IQGAP1_{FL}$, $IQGAP1_{\Delta NT}$, $IQGAP1_{2\text{-}522}$, $IQGAP1_{2\text{-}210}$, $IQGAP1_{2\text{-}71}$, or tau were mixed with 500 nM N-WASP. After a 1-hour incubation, beads were collected by centrifugation and washed, and bound proteins were analyzed by chemiluminescent immunoblotting.

Pyrene-actin assembly assay

Previously published methods were used to purify rabbit muscle actin (Bashour et al., 1997), and recombinant, his-tagged $IQGAP1_{FL}$, $IQGAP1_{\Delta NT}$, $IQGAP1_{2\text{-}522}$, $IQGAP1_{2\text{-}210}$ and $IQGAP1_{2\text{-}71}$ (Mateer et al., 2004). $IQGAP1_{\Delta NT}$ is a newly described deletion mutant derived from a pBlueScript II SK(+) plasmid containing the full-length human cDNA for IQGAP1 (pBSIQG1-MH) by the same methods used to create the other IQGAP1 deletion mutants used in this study. $IQGAP1_{\Delta NT}$ lacks only the first 156 amino acids of full-length IQGAP1, and was purified from baculovirus-infected Sf9 insect cells. Published methods were also used for purifying GST-VCA from bacteria (Egile et al., 1999), the Arp2/3 complex from bovine calf thymus (Higgs et al., 1999) and rat N-WASP from baculovirus-infected Sf9 cells (Miki et al., 1998), and for covalently coupling pyrene to purified actin (Bryan and Coluccio, 1985). Pyrene-actin assembly assays were performed in polymerization buffer (2 mM Tris, and 20 mM imidazole pH 7.5, 100 mM KCl, 2 mM $MgCl_2$, 1 mM EGTA, 0.1 mM EDTA, 1 mM DTT, 0.2 mM ATP and 0.2 mM PMSF) using 365 nm excitation and 386 nm emission in a Photon Technology Incorporated model QM-4/5000 spetrofluorometer. In each assay, 5% of the total actin was pyrene-labeled.

Prior to performing actin assembly assays by spectrofluorometry or TIRF microscopy, proteins were dialyzed overnight at 4°C in the following buffers: actin (2 mM Tris pH 8.0, 0.2 mM ATP, 0.1 mM DTT, 0.2 mM $CaCl_2$); the Arp2/3 complex (20 mM Tris pH 7.5, 50 mM KCl, 0.2 mM EGTA, 0.2 mM $MgCl_2$, 0.1 mM ATP, 0.5 mM DTT); all forms of IQGAP1 (50 mM Tris pH 7.5, 20 mM imidazole, 200 mM KCl, 1 mM EGTA, 0.1 mM ATP, 1 mM DTT, 0.1 mM PMSF); N-WASP (20 mM Tris pH 7.5, 10 mM EDTA, 0.1 mM PMSF). Following dialysis, insoluble protein was removed from each sample by centrifugation for 30 minutes at 4°C at 213,483 ***g*** (max.) in a Beckman TLA 120.1 rotor using a Beckman Optima TLX Ultracentrifuge. Next, the actin was mixed with EGTA to 1 mM and $MgCl_2$ to 0.1 mM, and then incubated for 2 minutes at room temperature. During this 2 minute period, the remaining proteins were mixed together, and the cocktail was adjusted with concentrated stock solutions of buffers, salts, ATP and PMSF to yield a final solution composition at pH 7.5 of 20 mM Tris, 20 mM imidazole, 100 mM KCl, 2 mM $MgCl_2$, 1 mM EGTA, 1 mM DTT, 0.2 mM ATP and 0.2 mM PMSF.

TIRF microscopy

Methods for preparing Oregon Green-labeled actin, and TIRF microscopy have been described previously (Kuhn and Pollard, 2005). Images were captured at 5-second intervals on an Olympus IX 71 inverted microscope using a 60×/1.45 NA Olympus objective, a Melles Griot 25 mW argon laser, a Roper CoolSNAP cooled CCD, and Scanalytics IP Lab software. Samples were prepared exactly as for pyrene-actin assembly assays, except that Oregon green-actin was used at 20% of total actin in place of 5% pyrene-actin. Sample chambers were coated with 6.25-25 nM *N*-ethylmaleimide-modified (Veigel et al., 1998) rabbit skeletal muscle myosin II (Sigma) prior to loading actin assembly cocktails into the chambers. TIRF experiments were typically terminated after 10 minutes, when substrate-bound actin filaments became so dense that it was no longer possible to resolve individual filaments.

This work was supported by NIH grants NS30485 and NS051746, and a University of Virginia Digestive Diseases Research Center Pilot/Feasibility Award through NIH P30 grant DK067629 to G.S.B.; and NIH grant GM067222 to D.A.S. The authors thank Scott Mateer and Leah Morris for their contributions to this project during its initial stages, Jean-Marie Sontag for designing the IQGAP1 fragments, Megan Bloom for assistance with the statistical analysis, and Ammasi (Peri) Periasamy for help with TIRF microscopy. We also thank Ruth Kroschewsky (ETH Zurich) and Marie-France Carlier (CNRS, Gif-sur-Yvette) for sharing data about their parallel study (Le Clainche et al., 2007) prior to publication.

References

Bashour, A.-M., Fullerton, A. T., Hart, M. J. and Bloom, G. S. (1997). IQGAP1, a Rac- and Cdc42-binding protein, directly binds and cross-inks microfilaments. *J. Cell Biol.* **137**, 1555-1566.

Benesch, S., Polo, S., Lai, F. P., Anderson, K. I., Stradal, T. E., Wehland, J. and Rottner, K. (2005). N-WASP deficiency impairs EGF internalization and actin assembly at clathrin-coated pits. *J. Cell Sci.* **118**, 3103-3115.

Binder, L. I., Frankfurter, A. and Rebhun, L. I. (1985). The distribution of tau in the nervous system. *J. Cell Biol.* **101**, 1371-1378.

Briggs, M. W. and Sacks, D. B. (2003). IQGAP proteins are integral components of cytoskeletal regulation. *EMBO Rep.* **4**, 571-574.

Brill, S., Li, S., Lyman, C. W., Church, D. M., Wasmuth, J. J., Weissbach, L., Bernards, A. and Snijders, A. (1996). The Ras GTPase-activating-protein-related human protein IQGAP2 harbors a potential actin binding domain and interacts with calmodulin and Rho family GTPases. *Mol. Cell. Biol.* **16**, 4869-4878.

Bryan, J. and Coluccio, L. M. (1985). Kinetic analysis of F-actin depolymerization in the presence of platelet gelsolin and gelsolin-actin complexes. *J. Cell Biol.* **101**, 1236-1244.

Cupit, L. D., Schmidt, V. A., Miller, F. and Bahou, W. F. (2004). Distinct PAR/IQGAP expression patterns during murine development: implications for thrombin-associated cytoskeletal reorganization. *Mamm. Genome* **15**, 618-629.

Egile, C., Loisel, T. P., Laurent, V., Li, R., Pantaloni, D., Sansonetti, P. J. and Carlier, M. F. (1999). Activation of the CDC42 effector N-WASP by the Shigella flexneri IcsA protein promotes actin nucleation by Arp2/3 complex and bacterial actin-based motility. *J. Cell Biol.* **146**, 1319-1332.

Fukata, M., Kuroda, S., Fujii, K., Nakamura, T., Shoji, I., Matsuura, Y., Okawa, K., Iwamatsu, A., Kikuchi, A. and Kaibuchi, K. (1997). Regulation of cross-linking activity of actin filament by IQGAP1, a target for Cdc42. *J. Biol. Chem.* **272**, 29579-29583.

Fukata, M., Kuroda, S., Nakagawa, M., Kawajiri, A., Itoh, N., Shoji, I., Matsuura, Y., Yonehara, S., Fujisawa, H., Kikuchi, A. et al. (1999). Cdc42 and Rac1 regulate the interaction of IQGAP1 with beta-catenin. *J. Biol. Chem.* **274**, 26044-26050.

Fukata, M., Watanabe, T., Noritake, J., Nakagawa, M., Yamaga, M., Kuroda, S., Matsuura, Y., Iwamatsu, A., Perez, F. and Kaibuchi, K. (2002). Rac1 and Cdc42 capture microtubules through IQGAP1 and CLIP-170. *Cell* **109**, 873-885.

Hart, M. J., Callow, M. G., Souza, B. and Polakis, P. (1996). IQGAP1, a calmodulin-binding protein with a RasGAP-related domain, is a potential effector for Cdc42Hs. *EMBO J.* **15**, 2997-3005.

Higgs, H. N., Blanchoin, L. and Pollard, T. D. (1999). Influence of the C terminus of Wiskott-Aldrich syndrome protein (WASp) and the Arp2/3 complex on actin polymerization. *Biochemistry* **38**, 15212-15222.

Hinz, B., Alt, W., Johnen, C., Herzog, V. and Kaiser, H. W. (1999). Quantifying lamella dynamics of cultured cells by SACED, a new computer-assisted motion analysis. *Exp. Cell Res.* **251**, 234-243.

Ho, H. Y., Rohatgi, R., Lebensohn, A. M., Le, M., Li, J., Gygi, S. P. and Kirschner, M. W. (2004). Toca-1 mediates Cdc42-dependent actin nucleation by activating the N-WASP-WIP complex. *Cell* **118**, 203-216.

Kuhn, J. R. and Pollard, T. D. (2005). Real-time measurements of actin filament polymerization by total internal reflection fluorescence microscopy. *Biophys. J.* **88**, 1387-1402.

Kuroda, S., Fukata, M., Kobayashi, K., Nakafuku, M., Nomura, N., Iwamatsu, A. and Kaibuchi, K. (1996). Identification of IQGAP as a putative target for the small GTPases, Cdc42 and Rac1. *J. Biol. Chem.* **271**, 23363-23367.

Kuroda, S., Fukata, M., Nakagawa, M., Fujii, K., Nakamura, T., Ookubo, T., Izawa, I., Nagase, T., Nomura, N., Tani, H. et al. (1998). Role of IQGAP1, a target of the small GTPases Cdc42 and Rac1, in regulation of E-cadherin- mediated cell-cell adhesion. *Science* **281**, 832-835.

Le Clainche, C., Schlaepfer, D., Ferrari, A., Klingauf, M., Grohmanova, K., Veligodskiy, A., Didry, D., Le, D., Egile, C., Carlier M. F., Kroschewski, R. (2007). IQGAP1 stimulates actin assembly through the N-WASP-Arp2/3 pathway. *J. Biol. Chem.* **282**, 426-423.

Li, R., Debreceni, B., Jia, B., Gao, Y., Tigyi, G. and Zheng, Y. (1999). Localization of the PAK1-, WASP-, and IQGAP1-specifying regions of Cdc42. *J. Biol. Chem.* **274**, 29648-29654.

Li, Z., McNulty, D. E., Marler, K. J., Lim, L., Hall, C., Annan, R. S. and Sacks, D. B. (2005). IQGAP1 promotes neurite outgrowth in a phosphorylation-dependent manner. *J. Biol. Chem.* **280**, 13871-13878.

Machesky, L. M., Atkinson, S. J., Ampe, C., Vandekerckhove, J. and Pollard, T. D. (1994). Purification of a cortical complex containing two unconventional actins from Acanthamoeba by affinity chromatography on profilin-agarose. *J. Cell Biol.* **127**, 107-115.

Mataraza, J. M., Briggs, M. W., Li, Z., Entwistle, A., Ridley, A. J. and Sacks, D. B. (2003). IQGAP1 promotes cell motility and invasion. *J. Biol. Chem.* **278**, 41237-41245.

Mateer, S. C. and Bloom, G. S. (2003). IQGAPs: integrators of the cytoskeleton, cell adhesion machinery and signaling networks. *Cell Motil. Cytoskeleton* **55**, 147-155.

Mateer, S. C., McDaniel, A. E., Nicolas, V., Habermacher, G. M., Lin, M.-J. S., Cromer, D. A., King, M. E. and Bloom, G. S. (2002). The mechanism for regulation of the F-actin binding activity of IQGAP1 by calcium/calmodulin. *J. Biol. Chem.* **277**, 12324-12333.

Mateer, S. C., Morris, L. E., Cromer, D. A., Benseñor, L. B. and Bloom, G. S. (2004). Actin filament binding by a monomeric IQGAP1 fragment with a single calponin homology domain. *Cell Motil. Cytoskeleton* **58**, 231-241.

McCallum, S. J., Wu, W. J. and Cerione, R. A. (1996). Identification of a putative effector of Cdc42Hs with high sequence similarity to the RasGAP-related protein IQGAP1 and a Cdc42Hs binding partner with similarity to IQGAP2. *J. Biol. Chem.* **271**, 21732-21737.

Miki, H. and Takenawa, T. (2003). Regulation of actin dynamics by WASP family proteins. *J. Biochem.* **134**, 309-313.

Miki, H., Sasaki, T., Takai, Y. and Takenawa, T. (1998). Induction of filopodium formation by a WASP-related actin-depolymerizing protein N-WASP. *Nature* **391**, 93-96.

Pollard, T. D. and Borisy, G. G. (2003). Cellular motility driven by assembly and disassembly of actin filaments. *Cell* **112**, 453-465.

Rohatgi, R., Ho, H. Y. and Kirschner, M. W. (2000). Mechanism of N-WASP activation by CDC42 and phosphatidylinositol **4**, 5-bisphosphate. *J. Cell Biol.* **150**, 1299-1310.

Rohatgi, R., Ma, L., Miki, H., Lopez, M., Kirchhausen, T., Takenawa, T. and Kirschner, M. W. (1999). The interaction between N-WASP and the Arp2/3 complex links Cdc42-dependent signals to actin assembly. *Cell* **97**, 221-231.

Roy, M., Li, Z. and Sacks, D. B. (2004). IQGAP1 binds ERK2 and modulates its activity. *J. Biol. Chem.* **279**, 17329-17337.

Roy, M., Li, Z. and Sacks, D. B. (2005). IQGAP1 is a scaffold for mitogen-activated protein kinase signaling. *Mol. Cell. Biol.* **25**, 7940-7952.

Schmidt, V. A., Scudder, L., Devoe, C. E., Bernards, A., Cupit, L. D. and Bahou, W. F. (2003). IQGAP2 functions as a GTP-dependent effector protein in thrombin-induced platelet cytoskeletal reorganization. *Blood* **101**, 3021-3028.

Suetsugu, S., Yamazaki, D., Kurisu, S. and Takenawa, T. (2003). Differential roles of WAVE1 and WAVE2 in dorsal and peripheral ruffle formation for fibroblast cell migration. *Dev. Cell* **5**, 595-609.

Takemoto, H., Doki, Y., Shiozaki, H., Imamura, H., Utsunomiya, T., Miyata, H., Yano, M., Inoue, M., Fujiwara, Y. and Monden, M. (2001). Localization of IQGAP1 is inversely correlated with intercellular adhesion mediated by e-cadherin in gastric cancers. *Int. J. Cancer* **91**, 783-788.

Veigel, C., Bartoo, M. L., White, D. C., Sparrow, J. C. and Molloy, J. E. (1998). The stiffness of rabbit skeletal actomyosin cross-bridges determined with an optical tweezers transducer. *Biophys. J.* **75**, 1424-1438.

Watanabe, T., Wang, S., Noritake, J., Sato, K., Fukata, M., Takefuji, M., Nakagawa, M., Izumi, N., Akiyama, T. and Kaibuchi, K. (2004). Interaction with IQGAP1 links APC to Rac1, Cdc42, and actin filaments during cell polarization and migration. *Dev. Cell* **7**, 871-883.

Weissbach, L., Bernards, A. and Herion, D. W. (1998). Binding of myosin essential light chain to the cytoskeleton-associated protein IQGAP1. *Biochem. Biophys. Res. Commun.* **251**, 269-276.

Welch, M. D., DePace, A. H., Verma, S., Iwamatsu, A. and Mitchison, T. J. (1997). The human Arp2/3 complex is composed of evolutionarily conserved subunits and is localized to cellular regions of dynamic actin filament assembly. *J. Cell Biol.* **138**, 375-384.

Yamaoka-Tojo, M., Ushio-Fukai, M., Hilenski, L., Dikalov, S. I., Chen, Y. E., Tojo, T., Fukai, T., Fujimoto, M., Patrushev, N. A., Wang, N. et al. (2004). IQGAP1, a novel VEGF receptor binding protein involved in reactive oxygen species-dependent endothelial migration and proliferation. *Circ. Res.* **95**, 276-283.

Yamashiro, S., Noguchi, T. and Mabuchi, I. (2003). Localization of two IQGAPs in cultured cells and early embryos of *Xenopus laevis*. *Cell Motil. Cytoskeleton* **55**, 36-50.

Yamazaki, D., Suetsugu, S., Miki, H., Kataoka, Y., Nishikawa, S., Fujiwara, T., Yoshida, N. and Takenawa, T. (2003). WAVE2 is required for directed cell migration and cardiovascular development. *Nature* **424**, 452-456.

Yan, C., Martinez-Quiles, N., Eden, S., Shibata, T., Takeshima, F., Shinkura, R., Fujiwara, Y., Bronson, R., Snapper, S. B., Kirschner, M. W. et al. (2003). WAVE2 deficiency reveals distinct roles in embryogenesis and Rac-mediated actin-based motility. *EMBO J.* **22**, 3602-3612.

Zhang, B., Wang, Z. X. and Zheng, Y. (1997). Characterization of the interactions between the small GTPase Cdc42 and its GTPase-activating proteins and putative effectors. Comparison of kinetic properties of Cdc42 binding to the Cdc42-interactive domains. *J. Biol. Chem.* **272**, 21999-22007.

Zhou, R., Guo, Z., Watson, C., Chen, E., Kong, R., Wang, W. and Yao, X. (2003). Polarized distribution of IQGAP proteins in gastric parietal cells and their roles in regulated epithelial cell secretion. *Mol. Biol. Cell* **14**, 1097-1108.

Supplementary Table 1. *Summary of one-way ANOVA analysis of kymographic data.* See Figure 2 and the Experimental Procedures section for further details.

Parameter	ANOVA (F value)	Groups	Post-Hoc Multiple Comparison
PROTRUSION FREQUENCY (protrusion/min)	F (3, 494)= 458.817 P<0.0005	scrRNA Before FGF2 vs. siRNA Before FGF2	P=0.768
		scrRNA Before FGF2 vs. scrRNA After FGF2	P <0.0005
		siRNA Before FGF2 vs siRNA After FGF2	P =0.885
PROTRUSION VELOCITY (μm/min)	F(3, 632)= 358.584 P<0.0005	scrRNA Before FGF2 vs. siRNA Before FGF2	P <0.0005
		scrRNA Before FGF2 vs. scrRNA After FGF2	P <0.0005
		siRNA Before FGF2 vs siRNA After FGF2	P =0.025
PROTRUSION PERSISTENCE (min)	F(3,905)=477.717 P<0.0005	scrRNA Before FGF2 vs. siRNA Before FGF2	P <0.0005
		scrRNA Before FGF2 vs. scrRNA After FGF2	P =1
		siRNA Before FGF2 vs siRNA After FGF2	P <0.0005

Supplementary Figure 1. *IQGAP1$_{\Delta NT}$ does not bind F-actin.* Polymerized actin, full length IQGAP1 and IQGAP1$_{\Delta NT}$ were centrifuged at low speed individually and in the indicated combinations, and the supernatants (S) and pellets (P) were analyzed by SDSPAGE. Under these conditions, neither full length IQGAP1 nor IQGAP1$_{\Delta NT}$ pelleted, and only a small fraction of the F-actin pelleted in the absence of other proteins. Most F-actin pelleted in the presence of full length IQGAP1, because IQGAP1 bound and cross-linked actin filaments into more readily sedimentable aggregates. In contrast, the amount of sedimentable F-actin was not increased by the presence of IQGAP1$_{\Delta NT}$, because IQGAP1$_{\Delta NT}$ was unable to bind and cross-link actin filaments.

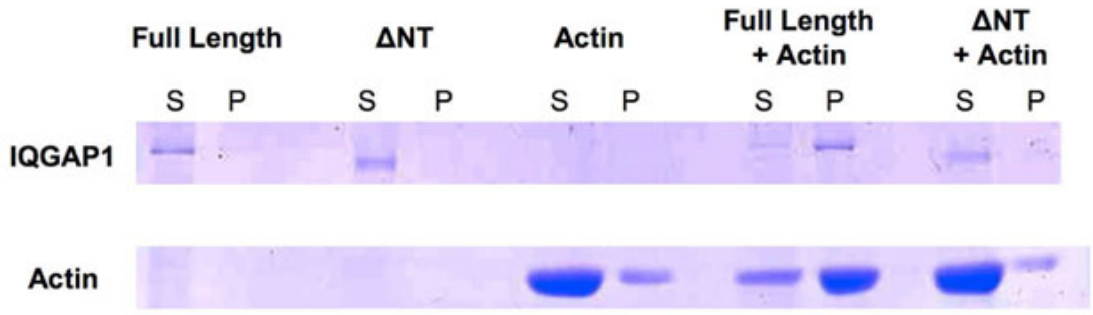

Supplementary Movie 1. *IQGAP1-stimulated assembly of branched actin filament networks observed directly by TIRF microscopy.* The movie corresponds to Figure 5C-E.

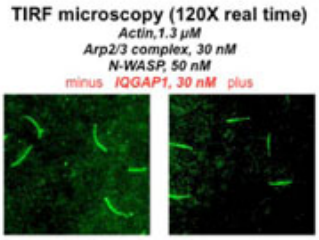

NOTE. This figure illustrates only the first frame of the movie, which must be downloaded separately. Viewing the movie requires QuickTime 7.0 or higher, which can be downloaded at no cost at the following URLs:
http://www.apple.com/quicktime/download/mac.html (Macintosh)
http://www.apple.com/quicktime/download/win.html (Windows)